# ALTERATIONS IN MITOCHONDRIAL AND LYSOSOMAL COMPARTMENTS UNDER CHEMOTHERAPY-INDUCED SENESCENCE

Shatalova RO, Shevyrev DV ✉

Translational Medicine Research Center, Sirius University of Science and Technology, Sirius Federal Territory, Krasnodar Krai, Russia

Cellular senescence is associated with the accumulation of senescent cells characterized by functional alterations, telomere shortening, cell cycle arrest, resistance to apoptosis, and metabolic dysregulation. In recent years, senescence has been extensively investigated not only in the context of aging but also in relation to cancer therapy, as senescence induction in various tumor cell types may differentially influence disease progression. The aim of this study was to comparatively evaluate commonly used chemotherapeutic agents with respect to their ability to induce senescence and their effects on mitochondrial and lysosomal compartments in primary dermal fibroblasts isolated from C57BL/6 mice. Cellular senescence was assessed using both chromogenic and fluorescent assays for β-galactosidase (β-Gal) activity. Mitochondria were labeled with the potential-sensitive dye MitoTracker® Orange, and lysosomes were stained with LysoTracker® Red. Flow cytometry analysis was performed using a BD LSRFortessa cytometer. Our results revealed a significant decrease in mitochondrial membrane potential and an increase in lysosomal fluorescence intensity in cells undergoing chemotherapy-induced senescence. Using an integrative senescence induction index developed in our laboratory, we demonstrated that doxorubicin exerts a more pronounced effect on senescence induction and on mitochondrial and lysosomal compartments compared to cisplatin, bleomycin, and etoposide.

**Keywords:** senescence, β-galactosidase, SA-β-Gal, mitochondria, lysosomes, doxorubicin, cisplatin, bleomycin, etoposide

**Funding:** This work was supported by Russian Science Foundation, Project No. 24-15-20003 (https://rscf.ru/project/24-15-20003/ accessed September 3, 2025).

**Author contribution:** Shatalova RO — optimization of cell culture conditions, cell staining; Shevyrev DV — manuscript preparation, flow cytometry experiments, cytometry data processing, statistical analysis, conceptualization.

**Compliance with ethical standards:** The study was approved by the Ethics Committee of Sirius University (Protocol No. 7.1, April 12, 2024) and conducted in accordance with the principles of the Declaration of Helsinki.

✉ **Correspondence should be addressed:** Daniil V. Shevyrev
1 Olimpiyskiy Avenue, Sochi, 354349, Russia; Email: dr.daniil25@mail.ru; shevyrev.dv@talantiuspeh.ru

**Received:** 06.09.2025 **Accepted:** 06.10.2025 **Published online:** 19.10.2025

**DOI:** 10.24075/brsmu.2025.045



# ИЗМЕНЕНИЯ МИТОХОНДРИАЛЬНОГО И ЛИЗОСОМНОГО КОМПАРТМЕНТОВ В УСЛОВИЯХ ХИМИОИНДУЦИРОВАННОЙ СЕНЕСЦЕНТНОСТИ

Р. О. Шаталова, Д. В. Шевырев ✉

Научный центр трансляционной медицины, Научно-технологический университет «Сириус», Федеральная территория «Сириус», Краснодарский край, Россия

Старение связано с накоплением сенесцентных клеток, для которых характерно изменение функций, укорочение теломер, остановка клеточного цикла, устойчивость к апоптозу и метаболические нарушения. В последние годы широко изучают различные аспекты сенесцентности не только в контексте старения, но и в отношении терапии опухолей, так как сенесцентность в различных клетках опухоли может по-разному влиять на ход патологического процесса. Целью исследования было провести сравнительный анализ распространенных химиотерапевтических препаратов в контексте индукции сенесцентности и влияния на митохондриальный и лизосомный компартменты фибробластов, выделенных из кожи мышей линии C57BL/6. Сенесцентность клеток оценивали с помощью хромогенного и флуоресцентного методов определения активности фермента β-Gal. Окрашивание митохондрий проводили с использованием потенциалзависимого красителя MitoTracker® Orange, лизосомы окрашивали с помощью LysoTracker® Red. Для анализа использовали проточный цитометр BD LSRFortessa. В результате было выявлено значительное снижение митохондриального потенциала и усиление интенсивности флуоресценции лизосом в клетках с химиоиндуцированной сенесцентностью. Использование разработанного нами интегрального индекса индукции сенесцентности позволило установить, что влияние доксорубицина с точки зрения индукции сенесцентности и влияния на митохондриальный и лизосомный компартменты выражено сильнее, чем у цисплатина, блеомицина и этопозида.

**Ключевые слова:** сенесцентность, β-галактозидаза, SA-β-Gal, митохондрии, лизосомы, доксорубицин, цисплатин, блеомицин, этопозид

**Финансирование:** данная работа выполнена при поддержке Российского Научного Фонда, проект № 24-15-20003 https://rscf.ru/project/24-15-20003/ (дата доступа 03 сентября 2025 г.).

**Вклад авторов:** Р. О. Шаталова — отработка условий культивирования, окрашивание клеток; Д. В. Шевырев — оформление рукописи, проведение проточной цитометрии, обработка данных цитометрии, статистическая обработка данных, концептуализация.

**Соблюдение этических стандартов:** исследование одобрено этическим комитетом университета «Сириус» (протокол заседания № 7.1 от 12 апреля 2024 г.), проведено в соответствии с требованиями Хельсинкской декларации.

✉ **Для корреспонденции:** Даниил Вадимович Шевырев
Олимпийский проспект, д. 1, г. Сочи, 354349, Россия; dr.daniil25@mail.ru; shevyrev.dv@talantiuspeh.ru

**Статья получена:** 06.09.2025 **Статья принята к печати:** 06.10.2025 **Опубликована онлайн:** 19.10.2025

**DOI:** 10.24075/vrgmu.2025.045

In recent years, interest in the study of cellular aging and senescence has markedly increased. The age-related accumulation of senescent cells impairs tissue homeostasis and, at the systemic level, contributes to chronic low-grade inflammation due to the secretion of a range of pro-inflammatory factors collectively known as the senescence-associated secretory phenotype (SASP) [1, 2]. In the context of oncogenesis, the role of senescence is dual: while it can halt tumor growth, it may simultaneously promote tumor cell survival and create a microenvironment conducive to metastasis [3, 4]. For instance, senescent tumor-associated fibroblasts generate a pro-inflammatory, angiogenic, and metabolically active niche that supports tumor survival and progression [5, 6]. Entry into senescence can be triggered by diverse stressors — ranging from replicative exhaustion to exposure to adverse physical, chemical, or biological agents — that induce various disruptions in the cellular molecular machinery [7]. Metabolic alterations in senescent cells are closely linked to mitochondrial dysfunction, a shift toward anaerobic glycolysis, and impaired autophagy [8, 9]. Specifically, downregulation of genes involved in mitochondrial fission (e.g., FIS1, DRP1, MFF) coupled with upregulation of fusion genes (MFN1, MFN2) disrupts mitochondrial dynamics in senescent cells [10, 11]. This results in mitochondrial mass expansion and the formation of an elongated, tubular mitochondrial network, which overall enhances resistance to oxidative stress via the PINK1-mediated pathway [12]. Such morphological changes are sometimes interpreted as an adaptive response to cellular stress. Notably, during the early stages of senescence, when mitochondrial aerobic activity is still preserved, the increased mitochondrial mass may lead to excessive production of reactive oxygen species (ROS). Consequently, this mitochondrial remodeling itself exacerbates cellular stress and contributes to the development of the pro-inflammatory SASP [13]. Progressive mitochondrial dysfunction is further characterized by diminished oxidative phosphorylation and a metabolic shift toward anaerobic glycolysis. This is reflected in a decline in mitochondrial membrane potential, reduced ATP production, and elevated ROS generation [14]. Excess ROS combined with ATP deficiency impairs the activity of vacuolar ATPase (v-ATPase), leading to lysosomal alkalinization and consequent dysfunction of acid hydrolases (e.g., proteases, lipases, nucleases) [15, 16]. As a result, autophagic efficiency declines, causing the accumulation of damaged proteins and organelles — including mitochondria — which further intensifies cellular stress [17]. Stress-induced activation of the PI3K/Akt pathway, autocrine signaling by SASP factors, and the buildup of damaged proteins converge to activate mTOR, which in turn suppresses TFEB — the master transcriptional regulator of lysosomal biogenesis and regeneration [18]. This suppression impairs autophagosome content degradation, leading to the accumulation of dysfunctional, alkalinized lysosomes that lose their degradative capacity and instead function primarily as storage compartments [15, 19]. Hypertrophy of the lysosomal compartment is accompanied by a compensatory increase in β-galactosidase activity, which becomes detectable at a suboptimal pH near 6.0 – hence termed senescence-associated β-galactosidase (SA-β-Gal) [20]. This enzymatic activity serves as a widely used biomarker for identifying senescent cells [21].

Currently, various models — both *in vivo* and *in vitro* — are employed to study cellular senescence. The aim of this study was to perform a comparative analysis of commonly used chemotherapeutic agents — doxorubicin, cisplatin, bleomycin, and etoposide — with respect to their capacity to induce senescence in primary mouse dermal fibroblast cultures. Additionally, we sought to characterize concomitant alterations in the mitochondrial and lysosomal compartments, as these organelles reflect critical aspects of the cell's metabolic and functional status and play a pivotal role in the establishment and maintenance of the senescent phenotype.

## METHODS

Primary dermal fibroblasts isolated from male C57BL/6 mice aged 4 and 19 months were used in this study. Animals were housed in a vivarium under a 12-hour light-dark cycle and provided *ad libitum* access to water and standard balanced laboratory chow. Euthanasia was performed in accordance with the principles of humane care for laboratory animals: under deep isoflurane-induced anesthesia followed by cervical dislocation. Biological samples were collected immediately after euthanasia. Cells derived from both young (4-month-old) and aged (19-month-old) mice were included in the analysis. However, preliminary experiments revealed no significant differences between fibroblasts from mice of different ages when compared at the same passage number; therefore, data from both age groups were pooled for subsequent analyses.

### Isolation of Dermal Fibroblasts

The dorsal skin was shaved using an animal trimmer, followed by disinfection with 70% ethanol for 2 minutes, allowing the alcohol to fully evaporate. A 2 × 2 cm skin fragment was aseptically excised using sterile scissors and immediately transferred into ice-cold phosphate-buffered saline (PBS) supplemented with 1% penicillin–streptomycin and 0.1% chlorhexidine for 5 minutes. The tissue was then rinsed with sterile PBS and placed in a Petri dish containing cold PBS. Using sterile instruments, subcutaneous adipose tissue was carefully removed. The dermal tissue was minced into fragments of approximately 1 $mm^2$. Enzymatic dissociation was performed in DMEM/F12 medium (PanEco, Russia) containing 0.2% collagenase IV (Gibco, USA) at 37 °C for 3 hours with periodic gentle agitation. Following incubation, enzymatic activity was neutralized by adding 100% fetal bovine serum (FBS; Capricorn Scientific, Germany) to a final concentration of 20%. The resulting cell suspension was filtered through a 40-μm cell strainer and centrifuged at 300g for 5 minutes. The pellet was gently resuspended and seeded into six-well tissue culture plates (Fudan Biotech, China) in DMEM/F12 medium supplemented with 10% FBS and 1% penicillin–streptomycin. Cells were maintained at 37 °C in a humidified atmosphere containing 5% $CO_2$ and subcultured upon reaching 85% confluence.

### Assessment of SA-β-Gal Activity

Senescence-associated β-galactosidase (SA-β-Gal) activity was evaluated using the chromogenic substrate 5-bromo-4-chloro-3-indolyl-β-D-galactopyranoside (X-Gal), which yields an intense blue precipitate upon enzymatic hydrolysis. Although β-galactosidase is constitutively present in lysosomes of most cell types and exhibits optimal activity at pH ~4.2, SA-β-Gal activity in senescent cells is detectable at a suboptimal pH of ~6.0 due to lysosomal hypertrophy and increased enzyme expression. To selectively identify senescent cells, staining was therefore performed at pH 6.0. Cells were washed with PBS and fixed with 0.2% glutaraldehyde for 10 minutes at room temperature, followed by three PBS washes. Staining was carried out in a solution containing: 2 mM citrate–phosphate buffer (pH 6.0), 50 mM potassium ferricyanide [$K_3Fe(CN)_6$],

50 mM potassium ferrocyanide [$K_4Fe(CN)_6$], 5 mM NaCl, 1 mM $MgCl_2$, and 20 mg/mL X-Gal (dissolved in DMSO; SibEnzyme, Russia). After addition of the staining solution, plates were incubated at 37 °C in ambient air for 20–24 hours. Cells were then washed twice with PBS and visualized using an AxioScope 5 light microscope (Carl Zeiss, Germany). The percentage of SA-β-Gal-positive (blue-stained) cells was determined manually by counting at least three microscopic fields from three independent wells per experimental condition.

For live-cell assessment of SA-β-Gal activity, the vital fluorescent probe SPiDER-βGal (Cellular Senescence Detection Kit, Dojindo Laboratories, Japan) was employed. Fibroblasts cultured in 24-well plates (NEST Biotechnology, China) were incubated for 1 hour at 37 °C in a $CO_2$ incubator with 1 mL of complete medium supplemented with bafilomycin A1 (final concentration as per manufacturer's instructions), which alkalinizes lysosomes by inhibiting vacuolar ATPase and thereby enhances probe retention and signal specificity. Subsequently, SPiDER-βGal was added to a final concentration of 1 μM, and cells were incubated under the same conditions for an additional hour. Excess probe was removed by PBS washes, and cells were detached using 0.25% trypsin–EDTA. Fluorescence intensity was quantified by flow cytometry using a BD LSRFortessa instrument (BD Biosciences, USA).

### Induction of Senescence

To induce senescence, we used chemotherapeutic agents commonly employed in the treatment of malignant diseases: doxorubicin, cisplatin, bleomycin, and etoposide. Doxorubicin is an anthracycline antitumor antibiotic whose mechanism of action involves intercalation between DNA strands and inhibition of topoisomerase II, leading to replication arrest. In addition, doxorubicin enhances the production of quinone-type free radicals and displaces histones from transcriptionally active chromatin [22]. Overall, its action results in DNA damage as well as transcriptomic and epigenetic disturbances. Cells are most sensitive to this drug during the S and G2 phases of the cell cycle [22]. Cisplatin is an alkylating cytotoxic agent that induces intra- and interstrand DNA crosslinks, thereby disrupting replication and transcription. Cisplatin causes cell cycle arrest at the G1, S, or G2 phase [23]. Bleomycin is an antitumor glycopeptide antibiotic that induces DNA strand breaks, presumably through the generation of free radicals. It blocks the cell cycle at the early G2 phase [24]. Etoposide is an antitumor agent that binds to topoisomerase II and inhibits its activity, preventing the resealing of DNA strand breaks normally introduced by topoisomerase II to relax DNA supercoils. Etoposide acts predominantly during the G2 and S phases of the cell cycle [25]. In general, these drugs induce genotoxic stress — one of the primary triggers of senescence.

Based on published data, a range of concentrations was selected for each inducer: 250, 350, and 450 nM for doxorubicin; 5, 10, and 20 μM for cisplatin; 10, 14, and 25 μM for bleomycin; and 5, 10, and 20 μM for etoposide. At medium and high concentrations, all inducers exhibited pronounced cytotoxic effects, resulting in the death of the majority of cells within the first 3–4 days of culture — conditions inconsistent with the aims of the study. Cell viability was assessed using an EVOS™ M5000 laser scanning microscope (Thermo Fisher Scientific, USA) with acridine orange (AO), which visualizes all nucleated cells, and propidium iodide (PI), which stains dead cells. At low doses, the cytotoxic effect was less pronounced; most cells survived and acquired morphological and biochemical features characteristic of senescence, as confirmed by X-Gal staining.

Ultimately, the lowest tested concentration for each inducer that maintained cell viability above 95% on day 7 was selected for further experiments. Fibroblasts were seeded into 24-well plates in DMEM/F12 medium (PanEco, Russia) supplemented with 10% FBS (Capricorn Scientific, Germany), 2 mM L-glutamine, and 1% penicillin–streptomycin (PanEco, Russia), and incubated at 37 °C in 5% $CO_2$ until they reached 60–70% confluence. The medium was then replaced with DMEM/F12 containing 1% FBS, and the inducers were added at the following final concentrations: 250 nM doxorubicin, 5 μM cisplatin, 10 μM bleomycin, and 5 μM etoposide. Cells were incubated under standard conditions for 24 hours, after which they were thoroughly washed and maintained for an additional 6 days in DMEM/F12 with 1% FBS, 2 mM L-glutamine, and 1% penicillin–streptomycin, with medium refreshed every three days. Control groups included cultures maintained in 10% FBS and in 1% FBS without any inducer. Subsequently, cells were processed for X-Gal staining, SPiDER-βGal labeling, and staining with MitoTracker® and LysoTracker® dyes.

### Mitochondrial and Lysosomal Staining

Mitochondria were stained in 24-well plates (NEST Biotechnology, China) using the potential-sensitive fluorescent dye MitoTracker® Orange CMTMRos (Invitrogen, USA) at a final concentration of 0.4 μM in DMEM/F12 medium supplemented with 1% FBS. Cells were incubated with the dye for 30 minutes at 37 °C in a 5% $CO_2$ atmosphere. MitoTracker Orange readily diffuses across the plasma membranes of live cells and selectively accumulates in active mitochondria in a membrane potential–dependent manner.

Lysosomes were stained under identical conditions using the acidotropic fluorescent probe LysoTracker® Red DND-99 (Invitrogen, USA) at a concentration of 50 nM. In neutral extracellular environments, LysoTracker Red freely crosses cellular membranes. Upon entering acidic compartments such as lysosomes, its weakly basic moiety becomes protonated, which prevents its diffusion back across the lysosomal membrane. This leads to selective retention and bright fluorescent labeling of acidic organelles.

Following staining, cells were detached using 0.25% trypsin–EDTA and immediately subjected to flow cytometry analysis.

### Statistical Analysis

Flow cytometry data were processed using BD FACSDiva software (v9.0) and FlowJo (v10.8.1). At least 500 events per sample were analyzed, with an average of 2,500 events per sample. Statistical analyses were performed using GraphPad Prism 9.3.1. Normality of data distribution was assessed using the Shapiro-Wilk and Kolmogorov-Smirnov tests. For normally distributed data, results are presented as mean ± standard deviation (Mean ± SD); for non-normally distributed data, results are reported as median with interquartile range (Me ± IQR). Multiple group comparisons were carried out using one-way analysis of variance (ANOVA), followed by Sidak's post hoc test for pairwise comparisons.

To comparatively evaluate the overall impact of the chemotherapeutic agents, we employed an integrative senescence induction index (IISI), which provides a composite assessment of the senescent phenotype by combining SA-β-Gal activity with concomitant alterations in mitochondrial and lysosomal parameters.

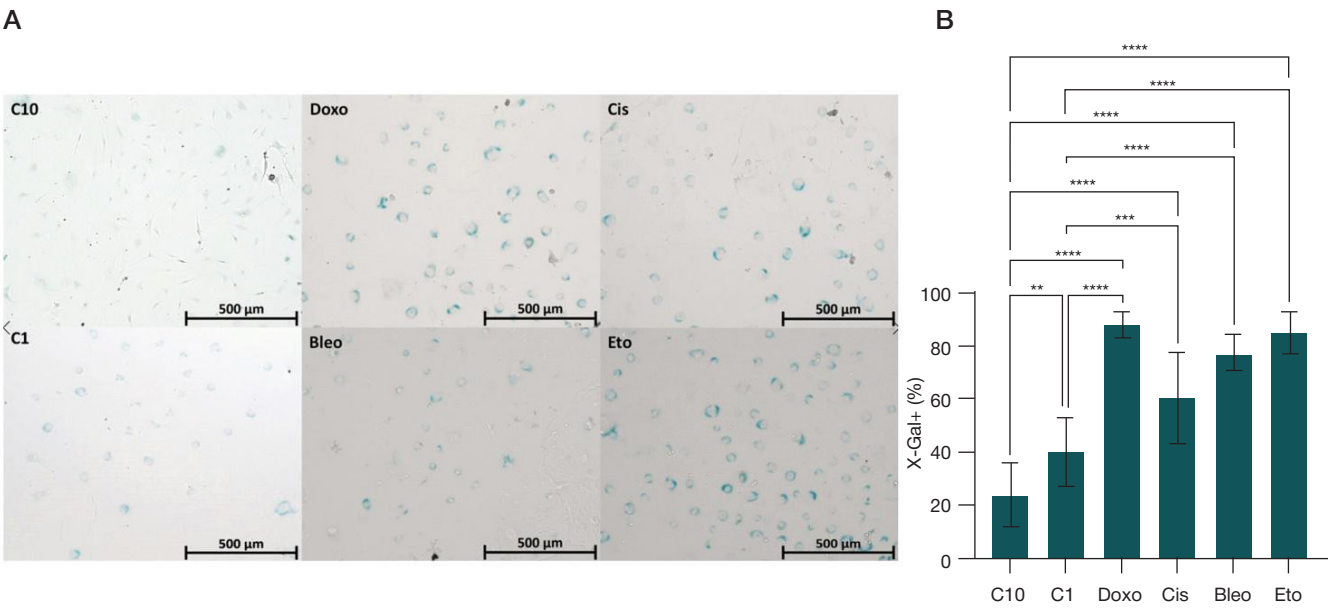


**Fig. 1. A**. Representative images of X-Gal chromogenic staining under different culture conditions. C10 — culture in 10% FBS; C1 — culture in 1% FBS; Doxo — doxorubicin; Cis — cisplatin; Bleo — bleomycin; Eto — etoposide. **B**. Comparative analysis of the proportion of SA-β-Gal–positive cells across experimental conditions (one-way ANOVA with Sidak's post hoc test; data pooled from nine microscopic fields across three independent wells per condition; Mean ± SD; ** — $p < 0.01$, *** — $p < 0.005$, **** — $p < 0.001$)

## RESULTS

Analysis of senescence induction in primary mouse dermal fibroblasts using the chromogenic substrate X-Gal revealed that all four tested agents – doxorubicin, cisplatin, bleomycin, and etoposide – significantly increased the proportion of senescent cells compared to the control group (Fig. 1).

Characteristic blue staining was predominantly localized in the perinuclear cytoplasm of fibroblasts and was uniformly observed across all inducer-treated groups (Fig. 1A). Notably, serum starvation alone also led to an increase in the proportion of SA-β-Gal–positive cells (39 ± 12%) compared to standard culture conditions with 10% FBS (23 ± 11%). Nevertheless, in all groups treated with senescence-inducing agents, the fraction of SA-β-Gal–positive cells was markedly higher, ranging from 60% to 87%. The highest level was observed with doxorubicin treatment, reaching 87.8 ± 4.5% (Fig. 1B).

At the next stage, senescence induction was assessed in live cells using the fluorogenic substrate SPiDER-βGal and flow cytometry. The gating threshold for SA-β-Gal–positive cells was established based on a negative control treated with bafilomycin A1 but without the addition of the SPiDER probe. The results obtained were consistent with those from X-Gal staining, and the distribution patterns of SA-β-Gal–positive cells under the different inducers were highly comparable between the two independent detection methods (Fig. 2A, B).

Assessment of the mitochondrial compartment revealed intriguing alterations (Fig. 2C, D). Fluorescence intensity in the MitoTracker detection channel (561–585/15 nm) was relatively high under standard culture conditions (10% FBS), but unexpectedly increased further under serum starvation (1% FBS). In contrast, treatment with senescence-inducing agents led to a significant and expected decrease in fluorescence intensity, reflecting a loss of mitochondrial membrane potential. This reduction was most pronounced in cells treated with doxorubicin.

Alterations were also observed in the lysosomal compartment. Under normal culture conditions (10% FBS) and serum starvation (1% FBS), fluorescence intensity in the LysoTracker detection channel (561–610/20 nm) remained comparable. However, upon treatment with senescence-inducing agents, a significant increase in lysosomal fluorescence was detected, indicating lysosomal hypertrophy. The most pronounced effects were observed with doxorubicin and etoposide (Fig. 2D, E).

To simultaneously evaluate the impact of each inducer across all three key parameters — the proportion of SA-β-Gal–positive cells, the reduction in mitochondrial membrane potential, and the degree of lysosomal hypertrophy — we developed an Integrative Index of Senescence Induction (IISI):

$$IISI = \frac{\%SPiDER_i^+}{\%SPiDER_{C1}^+} \times \left( \frac{MFI_{c10}mito}{MFI_imito} + \frac{MFI_ilyso}{MFI_{C10}lyso} \right),$$

where $\%SPiDER_i+$ and $\%SPiDER_{C1}+$ represent the percentage of SA-β-Gal–positive cells under a specific senescence inducer and under serum starvation (1% FBS), respectively; $MFI_{c10}mito$ and $MFImito$ denote the median fluorescence intensity (*MFI*) of MitoTracker in the control condition with 10% FBS and under senescence induction, respectively; $MFI_ilyso$ and $MFI_{C10}lyso$ denote the *MFI* of LysoTracker under senescence induction and in the 10% FBS control, respectively.

The application of the IISI enabled us to determine that, under our experimental conditions, doxorubicin exerted the strongest overall effect across all three parameters compared to the other tested inducers (Fig. 3).

Thus, we performed a comparative analysis of alterations in the mitochondrial and lysosomal compartments in primary mouse fibroblasts in the context of chemotherapy-induced senescence, demonstrating that doxorubicin exerted the most pronounced effect among the tested agents. Nevertheless, it should be noted that the Integrative Index of Senescence Induction (IISI) serves as a tool for relative comparison within the framework of this study, and its absolute numerical value is not intended for standalone interpretation.

## DISCUSSION

In the present study, using two independent senescence detection methods — chromogenic X-Gal staining and the fluorogenic substrate SPiDER — we confirmed that

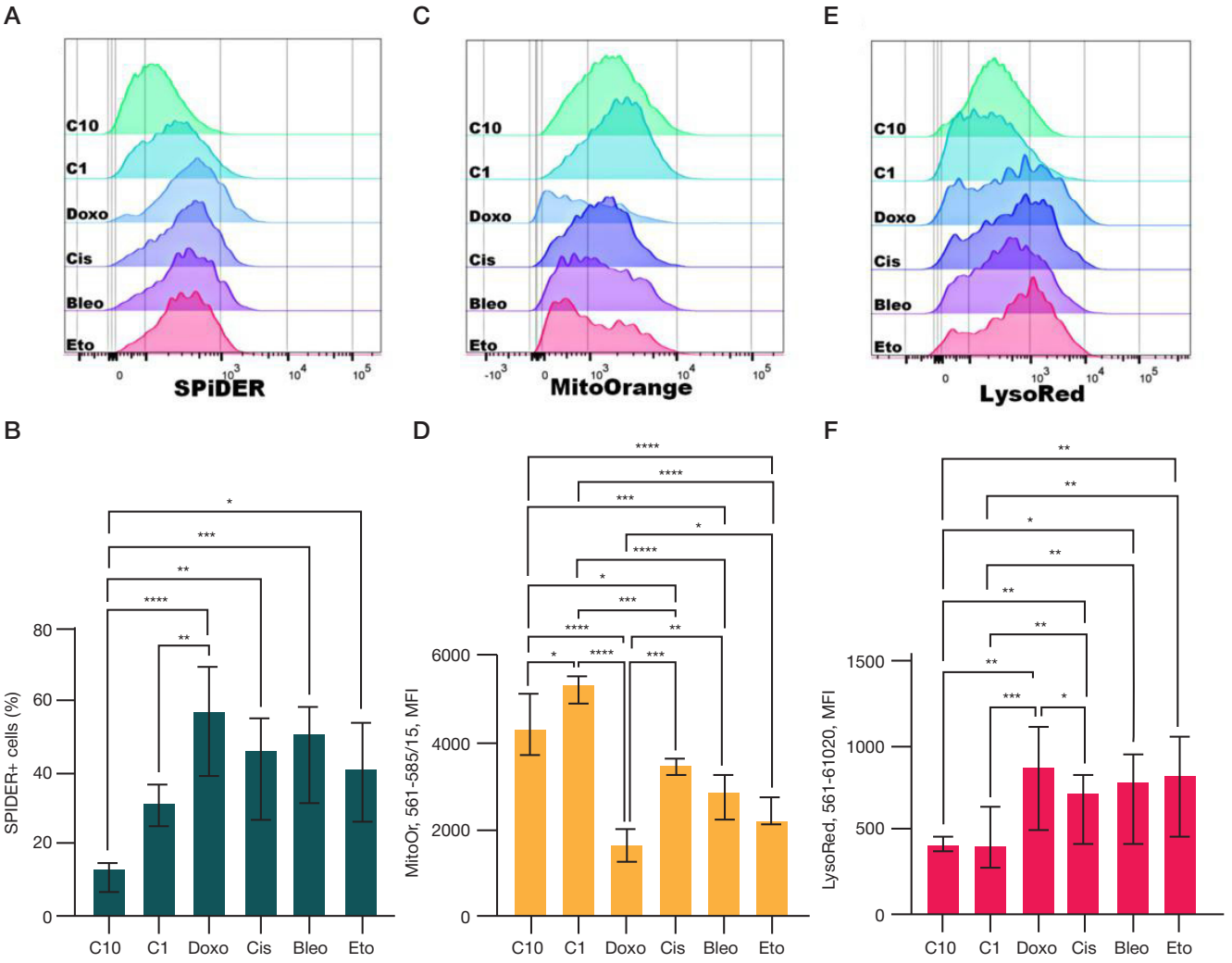


**Fig. 2.** The upper row shows representative histograms of SA-β-Gal–positive cells detected with SPiDER **(A)**, mitochondrial staining with MitoTracker Orange **(C)**, and lysosomal labeling with LysoTracker Red **(E)**. Histograms correspond to control conditions (C10 — culture in 10% FBS; C1 — culture in 1% FBS) and treatment with senescence inducers (Doxo — doxorubicin; Cis — cisplatin; Bleo — bleomycin; Eto — etoposide). Each histogram represents pooled data from four biological replicates per condition — two independent fibroblast isolations (from two individual mice), each analyzed in duplicate. Overall, the histograms illustrate an increase in the proportion of SA-β-Gal–positive cells, a reduction in mitochondrial membrane potential, and lysosomal hypertrophy in response to senescence-inducing agents, consistent with the results of statistical analysis. The lower row presents the corresponding quantitative analyses: percentage of SA-β-Gal–positive cells assessed by SPiDER fluorescence **(B)**; mitochondrial activity based on MitoTracker Orange signal intensity **(D)**; and lysosomal compartment size evaluated via LysoTracker Red fluorescence **(F)**. For each staining and experimental condition, the total sample size was $n = 12$ (six independent replicates per mouse, with fibroblasts derived from two mice). Replicates were processed on different days. Data are shown as median ± interquartile range (Me ± IQR); * — $p < 0.05$, ** — $p < 0.01$, *** — $p < 0.005$, **** — $p < 0.001$

doxorubicin, cisplatin, bleomycin, and etoposide significantly increase the proportion of SA-β-Gal–positive cells, indicative of chemotherapy-induced senescence [26]. The most pronounced effect was observed with doxorubicin, which markedly elevated the fraction of X-Gal–positive cells (87.8 ± 4.5%) and demonstrated the highest activity in the integrative assessment based on our newly developed Integrative Index of Senescence Induction (IISI).

Interestingly, serum starvation alone also led to an increase in SA-β-Gal–positive cells. This observation aligns with the notion that reduced mitogenic stimulation and proliferative activity can elicit phenotypic features of aging even in the absence of exogenous damaging agents [27]. This effect is likely attributable to the depletion of antioxidant systems normally present in serum — such as albumin, glutathione, ascorbic acid, and tocopherols [28]. Under prolonged serum-free conditions, the antioxidant capacity of the medium diminishes, while basal mitochondrial respiration continues to generate reactive oxygen species (ROS) that cannot be effectively neutralized. This accumulation of ROS may induce genotoxic stress and trigger the transition into a senescent state [28, 29]. Notably, serum starvation also resulted in a significant increase in fluorescence signal from the potential-sensitive mitochondrial dye MitoTracker Orange. This likely reflects an adaptive response to metabolic stress (due to reduced insulin levels in low-serum medium) through enhanced aerobic glycolysis [30, 31]. However, when senescence inducers were applied under the same low-serum conditions, a marked decrease in MitoTracker Orange signal was observed — especially with doxorubicin. This reduction is likely driven primarily by loss of mitochondrial membrane potential ($\Delta\Psi m$), which outweighs any potential increase in mitochondrial mass. Such a state is characteristic of stable senescence, where a large pool of dysfunctional mitochondria fails to sustain adequate ATP production, forcing the cell to rely on anaerobic glycolysis for energy [32, 33]. This metabolic shift is associated with the secretion of metabolic intermediates — such as lactate, pyruvate, and alanine — into the extracellular environment, which neighboring tumor cells can exploit as alternative energy sources [34].

Serum starvation *in vitro*, like other forms of metabolic stress and energy deficit, activates the transcription factor EB (TFEB) via AMPK activation and mTORC1 inhibition [35, 36]. TFEB activation promotes cellular adaptation by upregulating autophagy and lysosomal biogenesis, thereby recycling cellular components to supply energy and essential building blocks and maintain viability [37]. In our experiments, serum starvation did not significantly enhance LysoTracker Red signal, possibly due to efficient lysosomal turnover and biogenesis under these conditions [38, 39]. In contrast, all chemotherapeutic inducers caused a substantial increase in LysoTracker Red fluorescence, most likely reflecting significant lysosomal hypertrophy that outweighs any potential signal reduction due to lysosomal alkalinization (which would otherwise decrease accumulation of the acidotropic LysoTracker probe). Lysosomal enlargement is a hallmark of senescent cells, thought to compensate for impaired lysosomal function [40]. The strongest effect was again observed with doxorubicin. Together with the elevated proportion of SA-β-Gal–positive cells, this supports the concept that lysosomal accumulation is not merely a bystander phenomenon but a functional feature of the senescent state, reflecting the exhaustion of cellular adaptive reserves [41].

Doxorubicin exhibited the most robust effect across all evaluated parameters, surpassing the other agents. This is likely due to its multifaceted mechanism of action: DNA intercalation, topoisomerase II inhibition, ROS generation, and direct damage to mitochondrial DNA [22]. Consequently, doxorubicin emerged as the most potent senescence inducer in primary mouse dermal fibroblast cultures and demonstrated the most pronounced mitochondrial toxicity.

Modern oncology increasingly confronts the dual nature of many chemotherapeutic agents [42, 43]. While effectively halting tumor growth, these drugs may simultaneously initiate processes that promote recurrence, metastasis, and adverse side effects [44–46]. At the heart of this paradox appears to be the balance between direct cytotoxicity toward tumor cells and the induction of senescence — both within the tumor and in surrounding normal tissues [6, 45]. On one hand, therapy-induced senescence in the tumor microenvironment can support tumor cell survival by providing nutrients, promoting angiogenesis, and facilitating metastatic spread [5, 6]. On the other hand, senescence enforces a durable cell cycle arrest, and SASP-derived inflammatory factors can recruit immune cells, thereby enhancing immune-surveillance and potentially promoting clearance of senescent tumor cells [47–49]. Therefore, future in vitro and in vivo studies are needed to comprehensively evaluate not only the cytotoxic potential of anticancer agents but also their senogenic (senescence-inducing) and immunogenic profiles. Such integrated assessments will be crucial for optimizing therapeutic strategies that maximize tumor suppression while minimizing pro-tumorigenic and systemic side effects associated with therapy-induced senescence.

## CONCLUSIONS

In this study, we demonstrated that all tested chemotherapeutic agents — doxorubicin, cisplatin, bleomycin, and etoposide — effectively induce senescence in primary dermal fibroblasts isolated from C57BL/6 mice. This was confirmed by a significant increase in the proportion of SA-β-Gal–positive cells, consistently observed using both chromogenic X-Gal staining and the live-cell fluorogenic probe SPiDER-βGal. The most pronounced effect was elicited by doxorubicin, which induced a senescent phenotype in 87.5% of cells (as assessed by X-Gal staining). Serum starvation also increased the fraction of cells exhibiting senescence-like features, albeit to a considerably lesser extent than the pharmacological inducers. Concurrently with SA-β-Gal activation, we observed two hallmark features of the senescent state: a reduction in mitochondrial membrane potential and lysosomal hypertrophy. These alterations were most prominent following treatment with doxorubicin and etoposide. To enable a comprehensive comparison of the senescence-inducing efficacy of the tested compounds, we developed an Integrative Index of Senescence Induction (IISI), which combines three key parameters: the proportion of senescent cells, mitochondrial status, and lysosomal compartment integrity. According to this index, doxorubicin exhibited the strongest overall capacity to induce senescence across all evaluated metrics. These findings highlight substantial differences among commonly used chemotherapeutic agents in their ability to drive cellular senescence and identify doxorubicin as the most potent inducer in this experimental model.

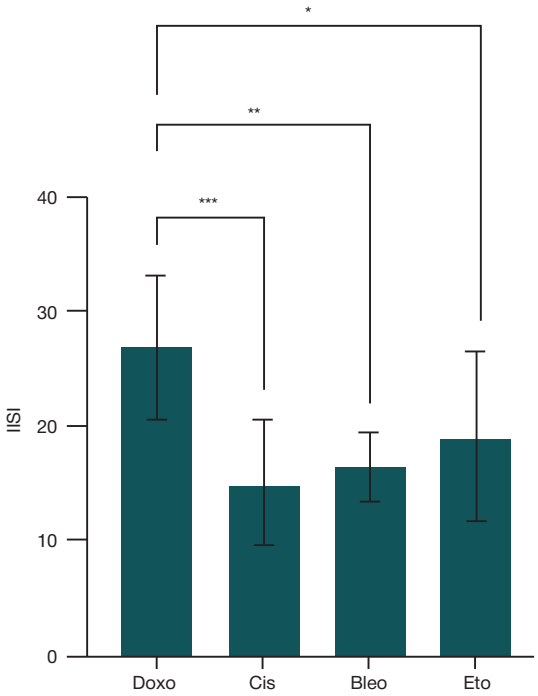


**Fig. 3.** Comparative analysis of the Integrative Index of Senescence Induction (IISI), which reflects the cumulative effect of each inducer across the three evaluated parameters: SA-β-Gal positivity, mitochondrial membrane potential loss, and lysosomal hypertrophy. Doxo — doxorubicin; Cis — cisplatin; Bleo — bleomycin; Eto — etoposide. Data are presented as Mean ± SD, $n = 8$; * — $p < 0.05$, ** — $p < 0.01$, *** — $p < 0.005$

Given that the tested agents elicited distinct senescence-associated phenotypes in fibroblasts, further investigation into their immunogenic profiles is warranted. Indeed, the immunomodulatory properties of chemotherapeutics — particularly their capacity to shape the tumor microenvironment via SASP-mediated immune cell recruitment or suppression — may be as therapeutically relevant as their direct cytotoxic effects. Understanding these nuances is essential for the rational design of immunologically informed cancer treatment strategies that balance tumor control with the mitigation of therapy-induced senescence–related complications.

**References**


1. Aquino-Martinez R, Eckhardt BA, Rowsey JL, Fraser DG, Khosla S, Farr JN, Monroe DG. Senescent cells exacerbate chronic inflammation and contribute to periodontal disease progression in old mice. J Periodontol. 2021; 92 (10): 1483–95. DOI: 10.1002/JPER.20-0529. Epub 2021 Jan 6. PMID: 33341947; PMCID: PMC8281492.
2. Tripathi U, Misra A, Tchkonia T, Kirkland JL. Impact of Senescent Cell Subtypes on Tissue Dysfunction and Repair: Importance and Research Questions. Mech Ageing Dev. 2021; 198: 111548. DOI: 10.1016/j.mad.2021.111548. Epub 2021 Aug 2. PMID: 34352325; PMCID: PMC8373827.
3. Schosserer M, Grillari J, Breitenbach M. The Dual Role of Cellular Senescence in Developing Tumors and Their Response to Cancer Therapy. Front Oncol. 2017; 7: 278. DOI: 10.3389/fonc.2017.00278. PMID: 29218300; PMCID: PMC5703792.
4. Ma L, Yu J, Fu Y, He X, Ge S, Jia R, et al. The dual role of cellular senescence in human tumor progression and therapy. MedComm (2020). 2024; 5 (9): e695. DOI: 10.1002/mco2.695. PMID: 39161800; PMCID: PMC11331035.
5. Coppé JP, Kauser K, Campisi J, Beauséjour CM. Secretion of vascular endothelial growth factor by primary human fibroblasts at senescence. J Biol Chem. 2006; 281 (40): 29568–74. DOI: 10.1074/jbc.M603307200. Epub 2006 Jul 31. PMID: 16880208.
6. Luo J, Sun T, Liu Z, Liu Y, Liu J, Wang S, et al. Persistent accumulation of therapy-induced senescent cells: an obstacle to long-term cancer treatment efficacy. Int J Oral Sci. 2025; 17 (1): 59. DOI: 10.1038/s41368-025-00380-w. PMID: 40750580; PMCID: PMC12317027.
7. Kumari R, Jat P. Mechanisms of Cellular Senescence: Cell Cycle Arrest and Senescence Associated Secretory Phenotype. Front Cell Dev Biol. 2021; 9: 645593. DOI: 10.3389/fcell.2021.645593. PMID: 33855023; PMCID: PMC8039141.
8. Sabbatinelli J, Prattichizzo F, Olivieri F, Procopio AD, Rippo MR, Giuliani A. Where Metabolism Meets Senescence: Focus on Endothelial Cells. Front Physiol. 2019; 10: 1523. DOI: 10.3389/fphys.2019.01523. PMID: 31920721; PMCID: PMC6930181.
9. Aman Y, Schmauck-Medina T, Hansen M, Morimoto RI, Simon AK, Bjedov I, Palikaras K, Simonsen A, Johansen T, Tavernarakis N, Rubinsztein DC, Partridge L, Kroemer G, Labbadia J, Fang EF. Autophagy in healthy aging and disease. Nat Aging. 2021; 1 (8): 634–50. DOI: 10.1038/s43587-021-00098-4. Epub 2021 Aug 12. PMID: 34901876; PMCID: PMC8659158.
10. Panfilova A, Zubareva T, Mironova E, Mazzoccoli G, Marasco MGP, Balazovskaia S, et al. Mitochondrial proteins as biomarkers of cellular senescence and age-associated diseases. Aging (Albany NY). 2025; 17. DOI: 10.18632/aging.206305. Epub ahead of print. PMID: 40856658.
11. Chen W, Zhao H, Li Y. Mitochondrial dynamics in health and disease: mechanisms and potential targets. Signal Transduct Target Ther. 2023; 8 (1): 333. DOI: 10.1038/s41392-023-01547-9. PMID: 37669960; PMCID: PMC10480456.
12. Murata H, Takamatsu H, Liu S, Kataoka K, Huh NH, Sakaguchi M. NRF2 Regulates PINK1 Expression under Oxidative Stress Conditions. PLoS One. 2015; 10 (11): e0142438. DOI: 10.1371/journal.pone.0142438. PMID: 26555609; PMCID: PMC4640816.
13. Zlotorynski E. Defective mitochondria ignite the SASP. Nat Rev Mol Cell Biol. 2020; 21 (4): 179. DOI: 10.1038/s41580-020-0228-x. PMID: 32076133.
14. Suski JM, Lebiedzinska M, Bonora M, Pinton P, Duszynski J, Wieckowski MR. Relation between mitochondrial membrane potential and ROS formation. Methods Mol Biol. 2012; 810: 183–205. DOI: 10.1007/978-1-61779-382-0_12. PMID: 22057568.
15. Li W, Kawaguchi K, Tanaka S, He C, Maeshima Y, Suzuki E, Toi M. Cellular senescence triggers intracellular acidification and lysosomal pH alkalinized via ATP6AP2 attenuation in breast cancer cells. Commun Biol. 2023; 6 (1): 1147. DOI: 10.1038/s42003-023-05433-6. PMID: 37993606; PMCID: PMC10665353.
16. Song Q, Meng B, Xu H, Mao Z. The emerging roles of vacuolar-type ATPase-dependent Lysosomal acidification in neurodegenerative diseases. Transl Neurodegener. 2020; 9 (1): 17. DOI: 10.1186/s40035-020-00196-0. PMID: 32393395; PMCID: PMC7212675.
17. Chung CY, Shin HR, Berdan CA, Ford B, Ward CC, Olzmann JA, et al. Covalent targeting of the vacuolar H+-ATPase activates autophagy via mTORC1 inhibition. Nat Chem Biol. 2019; 15 (8): 776–85. DOI: 10.1038/s41589-019-0308-4. Epub 2019 Jul 8. PMID: 31285595; PMCID: PMC6641988.
18. Omolekan TO, Chamcheu JC, Buerger C, Huang S. PI3K/AKT/mTOR Signaling Network in Human Health and Diseases. Cells. 2024; 13 (17): 1500. DOI: 10.3390/cells13171500. PMID: 39273070; PMCID: PMC11394329.
19. Loo TM, Zhou X, Tanaka Y, Sugawara S, Yamauchi S, Kawasaki H, et al. Senescence-associated lysosomal dysfunction impairs cystine deprivation-induced lipid peroxidation and ferroptosis. Nat Commun. 2025; 16 (1): 6617. DOI: 10.1038/s41467-025-61894-9. PMID: 40731111; PMCID: PMC12307602.
20. Kurz DJ, Decary S, Hong Y, Erusalimsky JD. Senescence-associated (beta)-galactosidase reflects an increase in lysosomal mass during replicative ageing of human endothelial cells. J Cell Sci. 2000; 113 (Pt 20): 3613–22. DOI: 10.1242/jcs.113.20.3613. PMID: 11017877.
21. Dimri GP, Lee X, Basile G, Acosta M, Scott G, Roskelley C, et al. A biomarker that identifies senescent human cells in culture and in aging skin in vivo. Proc Natl Acad Sci U S A. 1995; 92 (20): 9363–7. DOI: 10.1073/pnas.92.20.9363. PMID: 7568133; PMCID: PMC40985.
22. Kciuk M, Gielecińska A, Mujwar S, Kołat D, Kałuzińska-Kołat Ż, Celik I, et al. Doxorubicin-An Agent with Multiple Mechanisms of Anticancer Activity. Cells. 2023; 12 (4): 659. DOI: 10.3390/cells12040659. PMID: 36831326; PMCID: PMC9954613.
23. Dasari S, Tchounwou PB. Cisplatin in cancer therapy: molecular mechanisms of action. Eur J Pharmacol. 2014; 740: 364–78. DOI: 10.1016/j.ejphar.2014.07.025. Epub 2014 Jul 21. PMID: 25058905; PMCID: PMC4146684.
24. Dorr RT. Bleomycin pharmacology: mechanism of action and resistance, and clinical pharmacokinetics. Semin Oncol. 1992; 19 (2 Suppl 5): 3–8. PMID: 1384141.
25. Montecucco A, Zanetta F, Biamonti G. Molecular mechanisms of etoposide. EXCLI J. 2015; 14: 95–108. DOI: 10.17179/excli2015-561. PMID: 26600742; PMCID: PMC4652635.
26. Lubberts S, Meijer C, Demaria M, Gietema JA. Early ageing after cytotoxic treatment for testicular cancer and cellular senescence: Time to act. Crit Rev Oncol Hematol. 2020; 151: 102963. DOI: 10.1016/j.critrevonc.2020.102963. Epub 2020 May 7. PMID: 32446180.
27. Wiley CD, Campisi J. The metabolic roots of senescence: mechanisms and opportunities for intervention. Nat Metab. 2021; 3 (10): 1290–301. DOI: 10.1038/s42255-021-00483-8. Epub 2021 Oct 18. PMID: 34663974; PMCID: PMC8889622.
28. Zhang Y, Xu YY, Sun WJ, Zhang MH, Zheng YF, Shen HM, et al. FBS or BSA Inhibits EGCG Induced Cell Death through Covalent Binding and the Reduction of Intracellular ROS Production. Biomed Res Int. 2016; 2016: 5013409. DOI: 10.1155/2016/5013409. Epub 2016 Oct 18. PMID: 27830147; PMCID: PMC5088332.
29. Stival A, Silva A, Valadares M. Qualitative and quantitative evaluation of Fetal Bovine Serum composition: toward ethical and best quality in vitro science. NAM Journal. 2025. doi.org/10.1016/j.namjnl.2025.100047.
30. Liu Y, Birsoy K. Metabolic sensing and control in mitochondria. Mol Cell. 2023; 83 (6): 877–89. DOI: 10.1016/j.molcel.2023.02.016. PMID: 36931256; PMCID: PMC10332353.
31. Choi EJ, Oh HT, Lee SH, Zhang CS, Li M, Kim SY, et al. Metabolic stress induces a double-positive feedback loop between AMPK and SQSTM1/p62 conferring dual activation of AMPK and NFE2L2/NRF2 to synergize antioxidant defense. Autophagy. 2024; 20 (11): 2490–510. DOI: 10.1080/15548627.2024.2374692. Epub 2024 Jul 10. PMID: 38953310; PMCID: PMC11572134.
32. Fumagalli M, Rossiello F, Mondello C, d'Adda di Fagagna F. Stable cellular senescence is associated with persistent DDR activation. PLoS One. 2014; 9 (10): e110969. DOI: 10.1371/journal.pone.0110969. PMID: 25340529; PMCID: PMC4207795.

33. Ajoolabady A, Pratico D, Bahijri S, Eldakhakhny B, Tuomilehto J, Wu F, et al. Hallmarks and mechanisms of cellular senescence in aging and disease. Cell Death Discov. 2025; 11 (1): 364. DOI: 10.1038/s41420-025-02655-x. PMID: 40759632; PMCID: PMC12322153.
34. Dou X, Fu Q, Long Q, Liu S, Zou Y, Fu D, et al. PDK4-dependent hypercatabolism and lactate production of senescent cells promotes cancer malignancy. Nat Metab. 2023; 5 (11): 1887–910. DOI: 10.1038/s42255-023-00912-w. Epub 2023 Oct 30. Erratum in: Nat Metab. 2024; 6 (5): 980. DOI: 10.1038/s42255-024-01054-3. Erratum in: Nat Metab. 2024; 6 (7): 1416. DOI: 10.1038/s42255-024-01069-w. PMID: 37903887; PMCID: PMC10663165.
35. Hardie DG, Ross FA, Hawley SA. AMPK: a nutrient and energy sensor that maintains energy homeostasis. Nat Rev Mol Cell Biol. 2012; 13 (4): 251–62. DOI: 10.1038/nrm3311. PMID: 22436748; PMCID: PMC5726489.
36. Zhang S, Sheng H, Zhang X, Qi Q, Chan CB, Li L, et al. Cellular energy stress induces AMPK-mediated regulation of glioblastoma cell proliferation by PIKE-A phosphorylation. Cell Death Dis. 2019; 10 (3): 222. DOI: 10.1038/s41419-019-1452-1. Erratum in: Cell Death Dis. 2025; 16 (1): 447. DOI: 10.1038/s41419-025-07700-2. PMID: 30833542; PMCID: PMC6399291.
37. Shang L, Chen S, Du F, Li S, Zhao L, Wang X. Nutrient starvation elicits an acute autophagic response mediated by Ulk1 dephosphorylation and its subsequent dissociation from AMPK. Proc Natl Acad Sci U S A. 2011; 108 (12): 4788–93. DOI: 10.1073/pnas.1100844108. Epub 2011 Mar 7. PMID: 21383122; PMCID: PMC3064373.
38. Lee C, Lamech L, Johns E, Overholtzer M. Selective Lysosome Membrane Turnover Is Induced by Nutrient Starvation. Dev Cell. 2020; 55 (3): 289–97.e4. DOI: 10.1016/j.devcel.2020.08.008. Epub 2020 Sep 10. PMID: 32916093; PMCID: PMC8337093.
39. Ebner M, Puchkov D, López-Ortega O, Muthukottiappan P, Su Y, Schmied C, et al. Nutrient-regulated control of lysosome function by signaling lipid conversion. Cell. 2023; 186 (24): 5328–46.e26. DOI: 10.1016/j.cell.2023.09.027. Epub 2023 Oct 25. Erratum in: Cell. 2025; 188 (9): 2560. DOI: 10.1016/j.cell.2025.04.009. PMID: 37883971.
40. Hwang ES, Yoon G, Kang HT. A comparative analysis of the cell biology of senescence and aging. Cell Mol Life Sci. 2009; 66 (15): 2503–24. DOI: 10.1007/s00018-009-0034-2. Epub 2009 May 7. PMID: 19421842; PMCID: PMC11115533.
41. Tan JX, Finkel T. Lysosomes in senescence and aging. EMBO Rep. 2023; 24 (11): e57265. DOI: 10.15252/embr.202357265. Epub 2023 Oct 9. PMID: 37811693; PMCID: PMC10626421.
42. D'Alterio C, Scala S, Sozzi G, Roz L, Bertolini G. Paradoxical effects of chemotherapy on tumor relapse and metastasis promotion. Semin Cancer Biol. 2020; 60: 351–61. DOI: 10.1016/j.semcancer.2019.08.019. Epub 2019 Aug 24. PMID: 31454672.
43. Behranvand N, Nasri F, Zolfaghari Emameh R, Khani P, Hosseini A, Garssen J, Falak R. Chemotherapy: a double-edged sword in cancer treatment. Cancer Immunol Immunother. 2022; 71 (3): 507–26. DOI: 10.1007/s00262-021-03013-3. Epub 2021 Aug 5. Erratum in: Cancer Immunol Immunother. 2022; 71 (3): 527. DOI: 10.1007/s00262-021-03034-y. PMID: 34355266; PMCID: PMC10992618.
44. Middleton JD, Stover DG, Hai T. Chemotherapy-Exacerbated Breast Cancer Metastasis: A Paradox Explainable by Dysregulated Adaptive-Response. Int J Mol Sci. 2018; 19 (11): 3333. DOI: 10.3390/ijms19113333. PMID: 30373101; PMCID: PMC6274941.
45. Hwang HJ, Kang D, Shin J, Jung J, Ko S, Jung KH, et al. Therapy-induced senescent cancer cells contribute to cancer progression by promoting ribophorin 1-dependent PD-L1 upregulation. Nat Commun. 2025; 16 (1): 353. DOI: 10.1038/s41467-024-54132-1. PMID: 39753537; PMCID: PMC11699195.
46. Guillon J, Petit C, Toutain B, Guette C, Lelièvre E, Coqueret O. Chemotherapy-induced senescence, an adaptive mechanism driving resistance and tumor heterogeneity. Cell Cycle. 2019; 18 (19): 2385–97. DOI: 10.1080/15384101.2019.1652047. Epub 2019 Aug 9. PMID: 31397193; PMCID: PMC6738909.
47. Jiao D, Zheng X, Du X, Wang D, Hu Z, Sun R, et al. Immunogenic senescence sensitizes lung cancer to LUNX-targeting therapy. Cancer Immunol Immunother. 2022; 71 (6): 1403–17. DOI: 10.1007/s00262-021-03077-1. Epub 2021 Oct 21. PMID: 34674012; PMCID: PMC9123058.
48. Liu Y, Lomeli I, Kron SJ. Therapy-Induced Cellular Senescence: Potentiating Tumor Elimination or Driving Cancer Resistance and Recurrence? Cells. 2024; 13 (15): 1281. DOI: 10.3390/cells13151281. PMID: 39120312; PMCID: PMC11312217.
49. Marin I, Boix O, Garcia-Garijo A, Sirois I, Caballe A, Zarzuela E, et al. Cellular Senescence Is Immunogenic and Promotes Antitumor Immunity. Cancer Discov. 2023; 13 (2): 410–31. DOI: 10.1158/2159-8290.CD-22-0523. PMID: 36302218; PMCID: PMC7614152.


**Литература**


1. Aquino-Martinez R, Eckhardt BA, Rowsey JL, Fraser DG, Khosla S, Farr JN, Monroe DG. Senescent cells exacerbate chronic inflammation and contribute to periodontal disease progression in old mice. J Periodontol. 2021; 92 (10): 1483–95. DOI: 10.1002/JPER.20-0529. Epub 2021 Jan 6. PMID: 33341947; PMCID: PMC8281492.
2. Tripathi U, Misra A, Tchkonia T, Kirkland JL. Impact of Senescent Cell Subtypes on Tissue Dysfunction and Repair: Importance and Research Questions. Mech Ageing Dev. 2021; 198: 111548. DOI: 10.1016/j.mad.2021.111548. Epub 2021 Aug 2. PMID: 34352325; PMCID: PMC8373827.
3. Schosserer M, Grillari J, Breitenbach M. The Dual Role of Cellular Senescence in Developing Tumors and Their Response to Cancer Therapy. Front Oncol. 2017; 7: 278. DOI: 10.3389/fonc.2017.00278. PMID: 29218300; PMCID: PMC5703792.
4. Ma L, Yu J, Fu Y, He X, Ge S, Jia R, et al. The dual role of cellular senescence in human tumor progression and therapy. MedComm (2020). 2024; 5 (9): e695. DOI: 10.1002/mco2.695. PMID: 39161800; PMCID: PMC11331035.
5. Coppé JP, Kauser K, Campisi J, Beauséjour CM. Secretion of vascular endothelial growth factor by primary human fibroblasts at senescence. J Biol Chem. 2006; 281 (40): 29568–74. DOI: 10.1074/jbc.M603307200. Epub 2006 Jul 31. PMID: 16880208.
6. Luo J, Sun T, Liu Z, Liu Y, Liu J, Wang S, et al. Persistent accumulation of therapy-induced senescent cells: an obstacle to long-term cancer treatment efficacy. Int J Oral Sci. 2025; 17 (1): 59. DOI: 10.1038/s41368-025-00380-w. PMID: 40750580; PMCID: PMC12317027.
7. Kumari R, Jat P. Mechanisms of Cellular Senescence: Cell Cycle Arrest and Senescence Associated Secretory Phenotype. Front Cell Dev Biol. 2021; 9: 645593. DOI: 10.3389/fcell.2021.645593. PMID: 33855023; PMCID: PMC8039141.
8. Sabbatinelli J, Prattichizzo F, Olivieri F, Procopio AD, Rippo MR, Giuliani A. Where Metabolism Meets Senescence: Focus on Endothelial Cells. Front Physiol. 2019; 10: 1523. DOI: 10.3389/fphys.2019.01523. PMID: 31920721; PMCID: PMC6930181.
9. Aman Y, Schmauck-Medina T, Hansen M, Morimoto RI, Simon AK, Bjedov I, Palikaras K, Simonsen A, Johansen T, Tavernarakis N, Rubinsztein DC, Partridge L, Kroemer G, Labbadia J, Fang EF. Autophagy in healthy aging and disease. Nat Aging. 2021; 1 (8): 634–50. DOI: 10.1038/s43587-021-00098-4. Epub 2021 Aug 12. PMID: 34901876; PMCID: PMC8659158.
10. Panfilova A, Zubareva T, Mironova E, Mazzoccoli G, Marasco MGP, Balazovskaia S, et al. Mitochondrial proteins as biomarkers of cellular senescence and age-associated diseases. Aging (Albany NY). 2025; 17. DOI: 10.18632/aging.206305. Epub ahead of print. PMID: 40856658.
11. Chen W, Zhao H, Li Y. Mitochondrial dynamics in health and disease: mechanisms and potential targets. Signal Transduct Target Ther. 2023; 8 (1): 333. DOI: 10.1038/s41392-023-01547-9. PMID: 37669960; PMCID: PMC10480456.
12. Murata H, Takamatsu H, Liu S, Kataoka K, Huh NH, Sakaguchi M. NRF2 Regulates PINK1 Expression under Oxidative Stress Conditions. PLoS One. 2015; 10 (11): e0142438. DOI:

10.1371/journal.pone.0142438. PMID: 26555609; PMCID: PMC4640816.
13. Zlotorynski E. Defective mitochondria ignite the SASP. Nat Rev Mol Cell Biol. 2020; 21 (4): 179. DOI: 10.1038/s41580-020-0228-x. PMID: 32076133.
14. Suski JM, Lebiedzinska M, Bonora M, Pinton P, Duszynski J, Wieckowski MR. Relation between mitochondrial membrane potential and ROS formation. Methods Mol Biol. 2012; 810: 183–205. DOI: 10.1007/978-1-61779-382-0_12. PMID: 22057568.
15. Li W, Kawaguchi K, Tanaka S, He C, Maeshima Y, Suzuki E, Toi M. Cellular senescence triggers intracellular acidification and lysosomal pH alkalinized via ATP6AP2 attenuation in breast cancer cells. Commun Biol. 2023; 6 (1): 1147. DOI: 10.1038/s42003-023-05433-6. PMID: 37993606; PMCID: PMC10665353.
16. Song Q, Meng B, Xu H, Mao Z. The emerging roles of vacuolar-type ATPase-dependent Lysosomal acidification in neurodegenerative diseases. Transl Neurodegener. 2020; 9 (1): 17. DOI: 10.1186/s40035-020-00196-0. PMID: 32393395; PMCID: PMC7212675.
17. Chung CY, Shin HR, Berdan CA, Ford B, Ward CC, Olzmann JA, et al. Covalent targeting of the vacuolar H+-ATPase activates autophagy via mTORC1 inhibition. Nat Chem Biol. 2019; 15 (8): 776–85. DOI: 10.1038/s41589-019-0308-4. Epub 2019 Jul 8. PMID: 31285595; PMCID: PMC6641988.
18. Omolekan TO, Chamcheu JC, Buerger C, Huang S. PI3K/AKT/mTOR Signaling Network in Human Health and Diseases. Cells. 2024; 13 (17): 1500. DOI: 10.3390/cells13171500. PMID: 39273070; PMCID: PMC11394329.
19. Loo TM, Zhou X, Tanaka Y, Sugawara S, Yamauchi S, Kawasaki H, et al. Senescence-associated lysosomal dysfunction impairs cystine deprivation-induced lipid peroxidation and ferroptosis. Nat Commun. 2025; 16 (1): 6617. DOI: 10.1038/s41467-025-61894-9. PMID: 40731111; PMCID: PMC12307602.
20. Kurz DJ, Decary S, Hong Y, Erusalimsky JD. Senescence-associated (beta)-galactosidase reflects an increase in lysosomal mass during replicative ageing of human endothelial cells. J Cell Sci. 2000; 113 (Pt 20): 3613–22. DOI: 10.1242/jcs.113.20.3613. PMID: 11017877.
21. Dimri GP, Lee X, Basile G, Acosta M, Scott G, Roskelley C, et al. A biomarker that identifies senescent human cells in culture and in aging skin in vivo. Proc Natl Acad Sci U S A. 1995; 92 (20): 9363–7. DOI: 10.1073/pnas.92.20.9363. PMID: 7568133; PMCID: PMC40985.
22. Kciuk M, Gielecińska A, Mujwar S, Kołat D, Kałuzińska-Kołat Ż, Celik I, et al. Doxorubicin-An Agent with Multiple Mechanisms of Anticancer Activity. Cells. 2023; 12 (4): 659. DOI: 10.3390/cells12040659. PMID: 36831326; PMCID: PMC9954613.
23. Dasari S, Tchounwou PB. Cisplatin in cancer therapy: molecular mechanisms of action. Eur J Pharmacol. 2014; 740: 364–78. DOI: 10.1016/j.ejphar.2014.07.025. Epub 2014 Jul 21. PMID: 25058905; PMCID: PMC4146684.
24. Dorr RT. Bleomycin pharmacology: mechanism of action and resistance, and clinical pharmacokinetics. Semin Oncol. 1992; 19 (2 Suppl 5): 3–8. PMID: 1384141.
25. Montecucco A, Zanetta F, Biamonti G. Molecular mechanisms of etoposide. EXCLI J. 2015; 14: 95–108. DOI: 10.17179/excli2015-561. PMID: 26600742; PMCID: PMC4652635.
26. Lubberts S, Meijer C, Demaria M, Gietema JA. Early ageing after cytotoxic treatment for testicular cancer and cellular senescence: Time to act. Crit Rev Oncol Hematol. 2020; 151: 102963. DOI: 10.1016/j.critrevonc.2020.102963. Epub 2020 May 7. PMID: 32446180.
27. Wiley CD, Campisi J. The metabolic roots of senescence: mechanisms and opportunities for intervention. Nat Metab. 2021; 3 (10): 1290–301. DOI: 10.1038/s42255-021-00483-8. Epub 2021 Oct 18. PMID: 34663974; PMCID: PMC8889622.
28. Zhang Y, Xu YY, Sun WJ, Zhang MH, Zheng YF, Shen HM, et al. FBS or BSA Inhibits EGCG Induced Cell Death through Covalent Binding and the Reduction of Intracellular ROS Production. Biomed Res Int. 2016; 2016: 5013409. DOI: 10.1155/2016/5013409. Epub 2016 Oct 18. PMID: 27830147; PMCID: PMC5088332.
29. Stival A, Silva A, Valadares M. Qualitative and quantitative evaluation of Fetal Bovine Serum composition: toward ethical and best quality in vitro science. NAM Journal. 2025. doi.org/10.1016/j.namjnl.2025.100047.
30. Liu Y, Birsoy K. Metabolic sensing and control in mitochondria. Mol Cell. 2023; 83 (6): 877–89. DOI: 10.1016/j.molcel.2023.02.016. PMID: 36931256; PMCID: PMC10332353.
31. Choi EJ, Oh HT, Lee SH, Zhang CS, Li M, Kim SY, et al. Metabolic stress induces a double-positive feedback loop between AMPK and SQSTM1/p62 conferring dual activation of AMPK and NFE2L2/NRF2 to synergize antioxidant defense. Autophagy. 2024; 20 (11): 2490–510. DOI: 10.1080/15548627.2024.2374692. Epub 2024 Jul 10. PMID: 38953310; PMCID: PMC11572134.
32. Fumagalli M, Rossiello F, Mondello C, d'Adda di Fagagna F. Stable cellular senescence is associated with persistent DDR activation. PLoS One. 2014; 9 (10): e110969. DOI: 10.1371/journal.pone.0110969. PMID: 25340529; PMCID: PMC4207795.
33. Ajoolabady A, Pratico D, Bahijri S, Eldakhakhny B, Tuomilehto J, Wu F, et al. Hallmarks and mechanisms of cellular senescence in aging and disease. Cell Death Discov. 2025; 11 (1): 364. DOI: 10.1038/s41420-025-02655-x. PMID: 40759632; PMCID: PMC12322153.
34. Dou X, Fu Q, Long Q, Liu S, Zou Y, Fu D, et al. PDK4-dependent hypercatabolism and lactate production of senescent cells promotes cancer malignancy. Nat Metab. 2023; 5 (11): 1887–910. DOI: 10.1038/s42255-023-00912-w. Epub 2023 Oct 30. Erratum in: Nat Metab. 2024; 6 (5): 980. DOI: 10.1038/s42255-024-01054-3. Erratum in: Nat Metab. 2024; 6 (7): 1416. DOI: 10.1038/s42255-024-01069-w. PMID: 37903887; PMCID: PMC10663165.
35. Hardie DG, Ross FA, Hawley SA. AMPK: a nutrient and energy sensor that maintains energy homeostasis. Nat Rev Mol Cell Biol. 2012; 13 (4): 251–62. DOI: 10.1038/nrm3311. PMID: 22436748; PMCID: PMC5726489.
36. Zhang S, Sheng H, Zhang X, Qi Q, Chan CB, Li L, et al. Cellular energy stress induces AMPK-mediated regulation of glioblastoma cell proliferation by PIKE-A phosphorylation. Cell Death Dis. 2019; 10 (3): 222. DOI: 10.1038/s41419-019-1452-1. Erratum in: Cell Death Dis. 2025; 16 (1): 447. DOI: 10.1038/s41419-025-07700-2. PMID: 30833542; PMCID: PMC6399291.
37. Shang L, Chen S, Du F, Li S, Zhao L, Wang X. Nutrient starvation elicits an acute autophagic response mediated by Ulk1 dephosphorylation and its subsequent dissociation from AMPK. Proc Natl Acad Sci U S A. 2011; 108 (12): 4788–93. DOI: 10.1073/pnas.1100844108. Epub 2011 Mar 7. PMID: 21383122; PMCID: PMC3064373.
38. Lee C, Lamech L, Johns E, Overholtzer M. Selective Lysosome Membrane Turnover Is Induced by Nutrient Starvation. Dev Cell. 2020; 55 (3): 289–97.e4. DOI: 10.1016/j.devcel.2020.08.008. Epub 2020 Sep 10. PMID: 32916093; PMCID: PMC8337093.
39. Ebner M, Puchkov D, López-Ortega O, Muthukottiappan P, Su Y, Schmied C, et al. Nutrient-regulated control of lysosome function by signaling lipid conversion. Cell. 2023; 186 (24): 5328–46.e26. DOI: 10.1016/j.cell.2023.09.027. Epub 2023 Oct 25. Erratum in: Cell. 2025; 188 (9): 2560. DOI: 10.1016/j.cell.2025.04.009. PMID: 37883971.
40. Hwang ES, Yoon G, Kang HT. A comparative analysis of the cell biology of senescence and aging. Cell Mol Life Sci. 2009; 66 (15): 2503–24. DOI: 10.1007/s00018-009-0034-2. Epub 2009 May 7. PMID: 19421842; PMCID: PMC11115533.
41. Tan JX, Finkel T. Lysosomes in senescence and aging. EMBO Rep. 2023; 24 (11): e57265. DOI: 10.15252/embr.202357265. Epub 2023 Oct 9. PMID: 37811693; PMCID: PMC10626421.
42. D'Alterio C, Scala S, Sozzi G, Roz L, Bertolini G. Paradoxical effects of chemotherapy on tumor relapse and metastasis promotion. Semin Cancer Biol. 2020; 60: 351–61. DOI: 10.1016/j.semcancer.2019.08.019. Epub 2019 Aug 24. PMID: 31454672.
43. Behranvand N, Nasri F, Zolfaghari Emameh R, Khani P, Hosseini A, Garssen J, Falak R. Chemotherapy: a double-edged sword in cancer treatment. Cancer Immunol Immunother. 2022; 71 (3): 507–26. DOI: 10.1007/s00262-021-03013-3. Epub 2021 Aug 5. Erratum in: Cancer Immunol Immunother. 2022; 71 (3): 527. DOI: 10.1007/s00262-021-03034-y. PMID: 34355266; PMCID: PMC10992618.
44. Middleton JD, Stover DG, Hai T. Chemotherapy-Exacerbated Breast Cancer Metastasis: A Paradox Explainable by Dysregulated

Adaptive-Response. Int J Mol Sci. 2018; 19 (11): 3333. DOI: 10.3390/ijms19113333. PMID: 30373101; PMCID: PMC6274941.

45. Hwang HJ, Kang D, Shin J, Jung J, Ko S, Jung KH, et al. Therapy-induced senescent cancer cells contribute to cancer progression by promoting ribophorin 1-dependent PD-L1 upregulation. Nat Commun. 2025; 16 (1): 353. DOI: 10.1038/s41467-024-54132-1. PMID: 39753537; PMCID: PMC11699195.
46. Guillon J, Petit C, Toutain B, Guette C, Lelièvre E, Coqueret O. Chemotherapy-induced senescence, an adaptive mechanism driving resistance and tumor heterogeneity. Cell Cycle. 2019; 18 (19): 2385–97. DOI: 10.1080/15384101.2019.1652047. Epub 2019 Aug 9. PMID: 31397193; PMCID: PMC6738909.
47. Jiao D, Zheng X, Du X, Wang D, Hu Z, Sun R, et al. Immunogenic senescence sensitizes lung cancer to LUNX-targeting therapy. Cancer Immunol Immunother. 2022; 71 (6): 1403–17. DOI: 10.1007/s00262-021-03077-1. Epub 2021 Oct 21. PMID: 34674012; PMCID: PMC9123058.
48. Liu Y, Lomeli I, Kron SJ. Therapy-Induced Cellular Senescence: Potentiating Tumor Elimination or Driving Cancer Resistance and Recurrence? Cells. 2024; 13 (15): 1281. DOI: 10.3390/cells13151281. PMID: 39120312; PMCID: PMC11312217.
49. Marin I, Boix O, Garcia-Garijo A, Sirois I, Caballe A, Zarzuela E, et al. Cellular Senescence Is Immunogenic and Promotes Antitumor Immunity. Cancer Discov. 2023; 13 (2): 410–31. DOI: 10.1158/2159-8290.CD-22-0523. PMID: 36302218; PMCID: PMC7614152.